Lin Xiang, Xuhan Zhu, Fengcheng Pei, and Derrick Wing Kwan Ng, “Energy-Efficient Dynamic Array-Steering and Beamforming for UAV-Aided Communications” in *IEEE Global Communications Conference, Cape Town, South Africa, 2024.*

Energy-Efficient Dynamic Array-Steering and Beamforming for UAV-Aided Communications

Lin Xiang*, Xuhan Zhu*, Fengcheng Pei*, and Derrick Wing Kwan Ng†
*Technical University of Darmstadt †University of New South Wales
Emails: {l.xiang, f.pei}@nt.tu-darmstadt.de, xuhan.zhu@stud.tu-darmstadt.de, w.k.ng@unsw.edu.au

***Abstract*—In this paper, we explore energy-efficient designs for unmanned aerial vehicle (UAV)-aided communications, by employing a rotatable uniform linear array (ULA) of directional antennas, such as half-wavelength dipoles, onboard the UAV. Capitalizing on the kinematics of a rigid body, we derive a new analytical power consumption model for the mechanical steering of the dipole array. We then jointly optimize the transmit beamforming and array steering over time to maximize the system energy efficiency (EE), namely the ratio between the sum of spectral efficiency (SE) and the total power consumed in the UAV's propulsion flight, communication, and array steering, subject to constraints on transmit power and rotation speed. The formulated problem is highly nonconvex and generally intractable. Exploiting the underlying problem structure, we reformulate it into a parametric optimization involving convex and Stiefel manifold optimization subproblems, which are then solved leveraging a low-complexity block coordinate descent (BCD) algorithm. Simulation results demonstrate significant gains in system EE through the use of the dipole array and the joint optimization of transmit beamforming and array steering for UAV-aided communications. Besides, there exists an optimal number of transmit dipole antennas when employing the rotatable dipole array for UAV-aided communications to maximize the system EE.**

I. Introduction

Multi-antenna unmanned aerial vehicles (UAVs) offer a promising approach for delivering on-demand communication services to ground users in both standard and emergency scenarios [1]. Unlike terrestrial multi-antenna systems, these UAVs face unique challenges, including restricted size, weight, and power (SWAP), limited onboard antennas, and potential strong interference from undesired line-of-sight (LoS) links [2]. Therefore, developing spectral- and energy-efficient communication methods tailored for multi-antenna UAVs is of paramount importance [3].

To address these research problems, several studies have investigated the joint optimization of trajectory design and beamforming to maximize the sum of achievable data rates [4] or to minimize the energy consumption of UAVs [5], [6]. These strategies enable the UAVs to navigate toward favorable positions and channel conditions for mitigating pathloss, overcoming obstructions from obstacles in complex environments, and enhancing the performance gains of beamforming. The idea was further extended to cooperative trajectory and beamforming optimization involving multiple multi-antenna UAVs in [7]. However, these studies [4]–[7] primarily consider arrays of isotropic antennas for beamforming, neglecting the three-dimensional (3D) directional radiation pattern typical of practical communication antennas. To bridge this research gap, a more recent study [8] has investigated joint optimization of UAV trajectory and beamforming exploiting an array of directional antennas such as half-wavelength dipoles for minimizing the energy consumption of both flight and communication.

Meanwhile, unlike [4]–[8], the studies in [9], [10] have focused on hovering UAVs, while utilizing rotations of UAV or an additional gimbal device to flexibly steer the 3D orientation of the transmit antenna array. This approach is particularly beneficial for UAVs employing arrays of directional antennas. Indeed, upon this setting, array steering and beamforming can be jointly optimized to shape highly directive beams towards desired directions in 3D space and reduce interference leaked into undesired directions. Consequently, as demonstrated in [9], [10], this scheme enables highly spectral-efficient communications, even with a small number of antennas. However, the studies [9], [10] have overlooked the kinematics of mechanical array steering and the associated energy consumption that plays an important role in the system design. As our research will demonstrate, this oversight may jeopardize the energy efficiency (EE) of UAV-aided communication.

In this paper, we consider energy-efficient dynamic joint array steering and transmit beamforming designs for UAV-aided downlink communication that employs a rotatable array of directional antennas. However, to the best of our knowledge, the energy consumption associated with rotatable antenna arrays has not yet been investigated in the literature. To bridge this gap, we introduce, for the first time, a power consumption model for mechanical array steering, which is derived from the kinematics of a rigid body. We dynamically optimize array steering and beamforming over time to maximize system EE, defined as the ratio between the sum of spectral efficiency (SE) and the total power consumed in the UAV's propulsion flight, communication, and array steering, subject to constraints on transmit power and rotation speed. The formulated problem is highly nonconvex and more complex than those considered in [9], [10]. By exploiting the underlying problem structure, we reformulate it into a parametric optimization involving convex and Stiefel manifold optimization subproblems, which are further solved using a low-complexity iterative algorithm. Our contributions are

- We propose a practical kinematics-based analytical energy consumption model for UAV-aided communication employing a rotatable array of directional antennas.

This work has been funded by the LOEWE initiative (Hesse, Germany) within the emergenCITY center under grant LOEWE/1/12/519/03/05.001(0016)/72 and has been supported by the BMBF project Open6GHub under grant 16KISKO14 and by DAAD with funds from the German Federal Ministry of Education and Research (BMBF). The work of D. W. K. Ng is supported by the Australian Research Council's Discovery Projects (DP230100603, DP240101019).

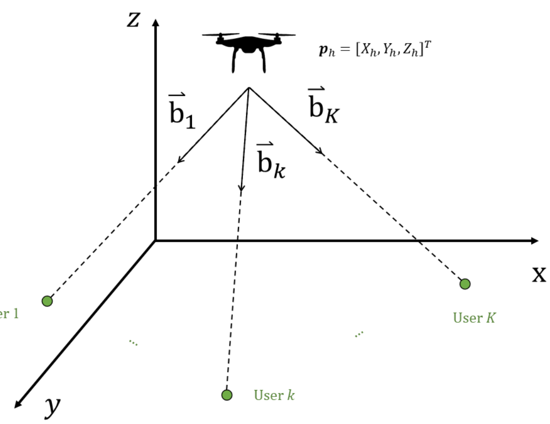

Fig. 1. System model of UAV-aided communications.

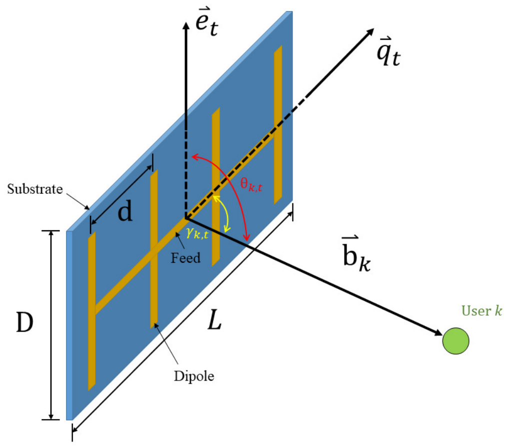

Fig. 2. Structure of the printed dipole array.

- We formulate a nonconvex problem to jointly optimize the array steering and beamforming over time for maximizing the system EE within constrained transmit power and rotation speed. We further propose a novel iterative block coordinate descent (BCD) algorithm to solve it.
- Simulation results show that significant gains in system EE can be achieved for UAV-aided communications by exploiting the dipole array as well as jointly optimizing transmit beamforming and array steering. Besides, the number of transmit dipole antennas needs to be judiciously optimized in order to maximize the system EE.

In the remainder of this paper, Section II presents the system model of multi-antenna UAV-aided communication. Sections III and IV present the problem formulation and the proposed solution for energy-efficient dynamic array-steering and beamforming, respectively. Section V presents the simulation results and, finally, Section VI concludes this paper.

Notations: Throughout this paper, vectors and matrices are denoted in boldface lower- and upper-case letters, respectively. $\mathbf{I}_N$ is the $N \times N$ identity matrix. $\mathbf{A}^T$ and $\mathbf{A}^H$ are the transpose and complex conjugate transpose of matrix $\mathbf{A}$, respectively. $(\cdot)^*$ represents the complex conjugate of a complex scalar and $\arccos(\cdot)$ denotes the inverse cosine function. Finally, $|\cdot|$ and $\|\cdot\|$ denote the modulus of a complex scalar and the Euclidean norm of a vector, respectively.

II. System Model

As shown in Fig. 1, an aerial base station (BS) enabled by a multi-antenna rotary-wing UAV aims to communicate with K single-antenna users in the downlink. User $k \in \mathcal{K} \triangleq \{1, \ldots, K\}$ is located at position $\mathbf{p}_k = [X_k, Y_k, Z_k]^T$. We assume that the UAV keeps hovering at position $\mathbf{p}_h = [X_h, Y_h, Z_h]^T$ while serving the users, so as to minimize the impact of Doppler shift during communication [11]. The UAV employs N_a half-wavelength dipole antennas arranged in a ULA for transmission. The dipole ULA is mounted onto the UAV adopting e.g. a three-axis (namely yaw, roll, and pitch) gimbal. This enables the dipole ULA to flexibly adjust both the 3D orientation and shape of the generated beams according to communication needs, with negligible impact on flight/hovering aerodynamics of the UAV. For convenience of modeling, we assume that the users are each equipped with a single isotropic receive antenna [8]–[10].

A. Joint Array Steering and Beamforming

The considered system operates in N radio frames indexed by $t \in \mathcal{T} \triangleq \{1, \ldots, N\}$. Each frame spans a duration of τ. The array orientation and radio resource allocation are controlled per frame. In particular, the array orientation in frame t is characterized by the axes of the antenna array and the element antenna, denoted by unit vectors $\vec{\mathbf{q}}_t \in \mathbb{R}^{3\times 1}$ and $\vec{\mathbf{e}}_t \in \mathbb{R}^{3\times 1}$, respectively, cf. Fig. 2. The arrow $\vec{\cdot}$ indicates that the vector is directional. We assume that the dipole axis $\vec{\mathbf{e}}_t$ is perpendicular to the array axis $\vec{\mathbf{q}}_t$. Let $\vec{\mathbf{b}}_k \triangleq (\mathbf{p}_k - \mathbf{p}_h) / \|\mathbf{p}_k - \mathbf{p}_h\|$ be the unit direction vector from the UAV's hovering position $\mathbf{p}_h$ to user k at position $\mathbf{p}_k$. Based on trigonometry, we have

$$\vec{\mathbf{b}}_k^T \cdot \vec{\mathbf{q}}_t = \cos \gamma_{k,t}, \quad \text{and} \tag{1}$$

$$\vec{\mathbf{b}}_k^T \cdot \vec{\mathbf{e}}_t = \cos \theta_{k,t}, \tag{2}$$

where $\gamma_{k,t}$ and $\theta_{k,t}$ are the angles extended by $\vec{\mathbf{b}}_k$ with respect to $\vec{\mathbf{q}}_t$ and $\vec{\mathbf{e}}_t$, respectively. For convenience, $\gamma_{k,t}$ and $\theta_{k,t}$ are referred to as the azimuth angle and the elevation angle of user k in frame t relative to the dipole array, respectively.

We consider a LoS channel between the elevated UAV and each user k in each frame t [8]–[10], which is modeled as

$$\mathbf{h}_{k,t} = \frac{\sqrt{\beta}}{\|\mathbf{p}_k - \mathbf{p}_h\|} \mathbf{a}_{k,t}, \tag{3}$$

where β is the reference value of path loss at the unit distance. Moreover, $\mathbf{a}_{k,t} \in \mathbb{R}^{N_a \times 1}$ is the steering vector of the dipole ULA for user k in frame t. For half-wavelength dipoles deployed in the ULA, we have [8], [9]

$$\mathbf{a}_{k,t} \triangleq F(\theta_{k,t}) \cdot [1, e^{j\pi \cos\gamma_{k,t}}, \ldots, e^{j\pi (N_a - 1)\cos\gamma_{k,t}}]^T, \tag{4}$$

where $F(\theta_{k,t})$ is the radiation pattern of each dipole, given by

$$F(\theta_{k,t}) = a_0 \cdot \frac{\cos\left(\frac{\pi}{2}\cos\theta_{k,t}\right)}{\sin\theta_{k,t}}, \tag{5}$$

and a_0 is a normalization coefficient to limit the total radiated power P_{rad} such that $P_{\mathrm{rad}} = \frac{1}{4\pi}\int_0^{\pi} F^2(\theta_{k,t}) \sin\theta_{k,t} d\theta_{k,t} = 1$.

Now, let $\mathbf{w}_{k,t} \in \mathbb{C}^{N_a \times 1}$ be the beamforming vector for transmitting signal $s_k \in \mathbb{C}$ to user $k \in \mathcal{K}$ in frame t. The transmit signal of the UAV in frame t is given as

$$\mathbf{s}_t = \sum\nolimits_{k=1}^{K} \mathbf{w}_{k,t} \cdot s_k. \tag{6}$$

We assume that s_k's are mutually uncorrelated random variables with unit power, that is $\mathbb{E}\{|s_k|^2\} = 1$ and $\mathbb{E}\{s_j^* s_k\} = 0, \forall j, k \in \mathcal{K}$ and $j \neq k$. The received signal of user k in frame t, denoted by $y_{k,t}$, is given as

$$y_{k,t} = \mathbf{h}_{k,t}^H \sum\nolimits_{k=1}^{K} \mathbf{w}_{k,t} \cdot s_k + n_{k,t}, \tag{7}$$

where $n_{k,t}$ is the received additive white Gaussian noise (AWGN) with zero mean and variance $\sigma_{k,t}^2$. The resulting achievable rate of user k in frame t is obtained as

$$R_{k,t} = \log_2\left(1 + \frac{|\mathbf{h}_{k,t}^H \mathbf{w}_{k,t}|^2}{\sum_{m=1, m\neq k}^{K} |\mathbf{h}_{k,t}^H \mathbf{w}_{m,t}|^2 + \sigma_{k,t}^2}\right). \tag{8}$$

B. Kinematics-based Power Consumption Model

1) Mechanical Steering Power: Following [12], we assume that the dipole array is printed on a thin rectangular substrate of length L and width D. The printed antenna array is controlled by the three-axis gimbal mounted on the UAV, where each of the three (yaw, roll, and pitch) axes is independently driven by a motor via a gearbox. According to the kinematics of rigid body [13], the moment of inertia of the printed dipole array about the $\vec{\mathbf{q}}_t$-axis and the $\vec{\mathbf{e}}_t$-axis through the center of mass is given by

$$I_q = \frac{1}{12} M D^2 \quad \text{and} \quad I_e = \frac{1}{12} M L^2, \tag{9}$$

respectively, where M is the mass of the printed dipole array. This requires a net work $\bar{W}_t$ to be done in rotating the rigid body, with

$$\bar{W}_t = \frac{1}{2} I_q v_{e,t}^2 + \frac{1}{2} I_e v_{q,t}^2, \tag{10}$$

where $v_{e,t} = \frac{1}{\tau}\arccos(\vec{\mathbf{e}}_t^T \vec{\mathbf{e}}_{t-1})$ and $v_{q,t} = \frac{1}{\tau}\arccos(\vec{\mathbf{q}}_t^T \vec{\mathbf{q}}_{t-1})$ denote the average angular velocity of $\vec{\mathbf{e}}_t$ and $\vec{\mathbf{q}}_t$ due to array steering in two consecutive frames, respectively. Consequently, we model the mechanical power consumption in frame t as the averaged power required for the net work done within the frame duration, which is derived as

$$\begin{aligned} P_{m,t} &= \frac{\bar{W}_t}{\tau} \\ &= \frac{M}{24\tau^3}\left[L^2 \arccos^2(\vec{\mathbf{q}}_t^T \vec{\mathbf{q}}_{t-1}) + D^2 \arccos^2(\vec{\mathbf{e}}_t^T \vec{\mathbf{e}}_{t-1})\right]. \end{aligned} \tag{11}$$

2) Total Power Consumption: Based on (11), the total power consumption P_{tot} in N frames is modeled as [14], [15]

$$P_{\text{tot}} = \sum\nolimits_{t=1}^{N} \left(P_{\text{stat}} + P_{b,t}\right) + \sum\nolimits_{t=2}^{N} \frac{1}{\eta_m \eta_g} P_{m,t}, \tag{12}$$

where P_{stat} is a constant to capture the UAV's power consumption caused by the circuitry and the propulsion for hovering. Moreover, $P_{b,t}$ is the power consumption for communication due to beamforming and associated signal processing on the radio frequency (RF) chains, as given by the first and second term, respectively. Further, $\eta_m \in (0,1]$ and $\eta_g \in (0,1]$ in (12) are the efficiency of the motor and the gearbox, respectively. When $\eta_m < 1$ and $\eta_g < 1$, an energy loss is incurred for conversion from electrical to mechanical energy in the motor and by friction in the gearbox, respectively. Assume that the power amplifier of the RF circuit operates in the linear region with a constant efficiency $\eta_0 \in (0,1]$ and each antenna element has a signal processing power P_{SP}. We model $P_{b,t}$ as

$$P_{b,t} = \frac{1}{\eta_0} \sum\nolimits_{k=1}^{K} \|\mathbf{w}_{k,t}\|^2 + N_a P_{\text{SP}}. \tag{13}$$

III. Problem Formulation

As the UAV usually has a limited battery, improving the energy utilization of the UAV during communication is crucial. To achieve this goal, in this section, we jointly optimize the mechanical steering $\{\vec{\mathbf{q}}_t, \vec{\mathbf{e}}_t\}_{t=1}^{N}$ and electrical beamforming $\{\mathbf{w}_t\}_{t=1}^{N}$ of the rotatable dipole ULA for maximizing the system EE η_{EE} (in bits/Hz/Joule) for all K users in N frames, defined as

$$\eta_{\text{EE}} \triangleq \frac{\sum_{t=1}^{N} \sum_{k=1}^{K} R_{k,t}}{P_{\text{tot}}}. \tag{14}$$

Specifically, η_{EE} is the ratio between the sum-SE (in bps/Hz) across N frames and the total power consumption (in W).

The resulting optimization problem is formulated as

$$\begin{aligned} \max_{\mathbf{w}_{k,t}, \vec{\mathbf{q}}_t, \vec{\mathbf{e}}_t} \quad & \eta_{\text{EE}} \\ \text{s.t.} \quad & \text{C1}: \|\mathbf{w}_{k,t}\|^2 \leq P_k, \quad k \in \mathcal{K}, \\ & \text{C2}: \|\vec{\mathbf{q}}_t\| = 1, \quad t \in \mathcal{T}, \\ & \text{C3}: \|\vec{\mathbf{e}}_t\| = 1, \quad t \in \mathcal{T}, \\ & \text{C4}: \vec{\mathbf{q}}_t^T \vec{\mathbf{e}}_t = 0, \quad t \in \mathcal{T}, \\ & \text{C5}: \vec{\mathbf{q}}_t^T \vec{\mathbf{q}}_{t-1} \geq \delta_1, \quad t \in \mathcal{T} \setminus \{1\}, \\ & \text{C6}: \vec{\mathbf{e}}_t^T \vec{\mathbf{e}}_{t-1} \geq \delta_2, \quad t \in \mathcal{T} \setminus \{1\}. \end{aligned} \tag{15}$$

Here, constraint C1 denotes the transmit power budget of user k, where $\sum_{k=1}^{K} P_k = P_{\max}$ and $P_{\max}$ is the maximum transmit power of the UAV. Besides, C2, C3, and C4 together ensure that the direction vectors $\vec{\mathbf{q}}_t$ and $\vec{\mathbf{e}}_t$ are orthonormal during array steering. Finally, C5 and C6 limit the maximal angular velocity of $\vec{\mathbf{q}}_t$ and $\vec{\mathbf{e}}_t$ per frame by $\arccos(\delta_1)$ and $\arccos(\delta_2)$, respectively, where $\delta_1, \delta_2 \in [-1, 1]$ are constants. Note that C2 and C3 also imply that $\vec{\mathbf{q}}_t^T \vec{\mathbf{q}}_{t-1} \leq 1$ and $\vec{\mathbf{e}}_t^T \vec{\mathbf{e}}_{t-1} \leq 1$, for which the latter requirements are ignored in C5 and C6. Additionally, although P_ks are assumed to be fixed in C1, they can also be optimized using our proposed solution.

Problem (15) is nonconvex due to the nonconvex objective function and nonconvex constraints C2, C3, C4, C5, and C6 associated with array steering. This type of problem is generally intractable, for which it is difficult to find its global optimal solutions with a polynomial-time computational complexity. As a compromise, in Section IV, we propose a low-complexity suboptimal solution to problem (15) by reformulating it as a parametric optimization using the Dinkelbach method [16]. The latter is further tackled by the proposed BCD algorithm.

IV. Problem Solution

A. Equivalent Problem Reformulation

Problem (15) is a nonconvex nonlinear fractional program, which is inconvenient to solve in its current form. To facilitate the solution development, we first transform (15) into a parameterized family of problems indexed by parameter $\vartheta \geq 0$,

$$\begin{aligned} \min_{u_{k,t}, x_{k,t}, \mathbf{w}_{k,t}, \vec{\mathbf{q}}_t, \vec{\mathbf{e}}_t} \quad & f(u_{k,t}, x_{k,t}, \mathbf{w}_{k,t}, \vec{\mathbf{q}}_t, \vec{\mathbf{e}}_t \mid \vartheta) \\ \text{s.t.} \quad & \text{C1} - \text{C6}, \end{aligned} \tag{16}$$

where the objective function is defined as

$$\begin{aligned} f(u_{k,t}, x_{k,t}, \mathbf{w}_{k,t}, \vec{\mathbf{q}}_t, \vec{\mathbf{e}}_t \mid \vartheta) &\triangleq \vartheta P_{\text{tot}} \\ &+ \sum\nolimits_{t=1}^{N} \sum\nolimits_{k=1}^{K} (x_{k,t} r_{k,t} + \log_2 x_{k,t}), \end{aligned} \tag{17}$$

$u_{k,t} \in \mathbb{C}$ and $x_{k,t} \in \mathbb{R}$ are auxiliary optimization variables, and $r_{k,t}$ denotes the mean square error (MSE) for estimating the transmit signal s_k from the received signal $y_{k,t}$ in (6) in frame t and is given as [17]

$$\begin{aligned} r_{k,t} \triangleq & |u_{k,t} \mathbf{h}_{k,t}^H \mathbf{w}_{k,t} - 1|^2 \\ &+ \sum\nolimits_{m=1, m \neq k}^{K} |u_{k,t} \mathbf{h}_{k,t}^H \mathbf{w}_{m,t}|^2 + |u_{k,t}|^2 \sigma_{k,t}^2. \end{aligned} \tag{18}$$

Hence, problem (16) can be interpreted as a sum-MSE minimization regularized by the total power consumption, where ϑ is the regularization parameter. In order to properly select the value of ϑ, we have the following lemma.

Lemma 1: Let $f^*(\vartheta)$ be the optimal objective value of problem (16) for given parameter $\vartheta \geq 0$. When $f^*(\vartheta) = 0$ for some $\vartheta \geq 0$, problem (16) is *equivalent* to the original problem (15) in the sense that the optimal solutions of both problems are identical.

Proof: By applying the Dinkelbach method [16], we rewrite problem (15) into a parametric optimization problem indexed by parameter $\vartheta \geq 0$,

$$\begin{aligned} \max_{\mathbf{w}_{k,t}, \vec{\mathbf{q}}_t, \vec{\mathbf{e}}_t} \quad & \sum\nolimits_{t=1}^{N} \sum\nolimits_{k=1}^{K} R_{k,t} - \vartheta P_{\text{tot}} \\ \text{s.t.} \quad & \text{C1} - \text{C6}. \end{aligned} \tag{19}$$

Problem (19) and (15) are equivalent if and only if the optimal objective value of problem (19), denoted by $g(\vartheta)$, satisfies $g(\vartheta) = 0$ [16].

We now show that problem (19) and (16) are equivalent. To this end, observe that problem (16) involves an unconstrained optimization over $u_{k,t}$ and $x_{k,t}$. Thus, the optimal solutions of $u_{k,t}$ and $x_{k,t}$, denoted by $u_{k,t}^*$ and $x_{k,t}^*$, can be obtained based on the first-order optimality conditions of problem (16). By setting $\partial f / \partial u_{k,t} = 0$ and $\partial f / \partial x_{k,t} = 0$, we have

$$u_{k,t}^* = \frac{\mathbf{h}_{k,t}^H \mathbf{w}_{k,t}}{\sum_{m=1}^{K} |\mathbf{h}_{k,t}^H \mathbf{w}_{m,t}|^2 + \sigma_{k,t}^2}, \quad \text{and} \tag{20}$$

$$x_{k,t}^* = r_{k,t}^{-1}. \tag{21}$$

Note that $u_{k,t}^*$ is virtually a minimum MSE (MMSE) receiver. Substituting (20) and (21) into (17), we have $f(u_{k,t}^*, x_{k,t}^*, \mathbf{w}_{k,t}, \vec{\mathbf{q}}_t, \vec{\mathbf{e}}_t \mid \vartheta) = \sum_{t=1}^{N} \vartheta P_{\text{tot}} - \sum_{k=1}^{K} R_{k,t}$. Thus, problem (19) and (16) are equivalent, with $f^*(\vartheta) + g(\vartheta) = 0$ for any $\vartheta \geq 0$. The latter implies that problem (16) is equivalent to (15) if and only if $f^*(\vartheta) = 0$, which completes the proof. ■

Based on Lemma 1, instead of solving problem (15), we can (i) find a suitable parameter ϑ and (ii) solve problem (16) for such ϑ. In the following, we start with addressing (ii) for any given ϑ using a low-complexity iterative solution, based on which (i) is further solved using the Dinkelbach method.

B. Proposed Iterative Optimization Solution

Note that the optimal solutions of $u_{k,t}$ and $x_{k,t}$ in problem (16) have been obtained in (20) and (21). In the following, we optimize $\{\mathbf{w}_{k,t}, \vec{\mathbf{q}}_t, \vec{\mathbf{e}}_t\}$ for given $\vartheta \geq 0$ using an iterative proximal BCD method. The latter decomposes the optimization variables into two blocks, i.e., $\{\mathbf{w}_{k,t}\}$ and $\{\vec{\mathbf{q}}_t, \vec{\mathbf{e}}_t\}$, and alternately optimize them until reaching convergence. In particular, the beamforming optimization subproblem for given $\{u_{k,t}, x_{k,t}\}$ and $\{\vec{\mathbf{q}}_t, \vec{\mathbf{e}}_t\}$ is formulated as

$$\begin{aligned} \min_{\mathbf{w}_{k,t} \in \mathbb{C}^{N_a \times 1}} \quad & f(\mathbf{w}_{k,t}; u_{k,t}, x_{k,t}, \vec{\mathbf{q}}_t, \vec{\mathbf{e}}_t \mid \vartheta) \\ \text{s.t.} \quad & \text{C1}. \end{aligned} \tag{22}$$

Meanwhile, the array steering optimization problem for given $\{u_{k,t}, x_{k,t}\}$ and $\{\mathbf{w}_{k,t}\}$ is formualted as

$$\begin{aligned} \min_{\vec{\mathbf{q}}_t, \vec{\mathbf{e}}_t \in \mathbb{R}^{3 \times 1}} \quad & f(\vec{\mathbf{q}}_t, \vec{\mathbf{e}}_t; u_{k,t}, x_{k,t}, \mathbf{w}_{k,t} \mid \vartheta) \\ \text{s.t.} \quad & \text{C2} - \text{C6}. \end{aligned} \tag{23}$$

With a slight abuse of notation, we have moved ahead the optimization variables in (22) and (23), to be before a semicolon.

The advantages of the BCD method lie in that it can exploit the special structures underlying the decomposed subproblems for convenient solution. For example, problem (22) is a convex optimization problem, which can be conveniently solved adopting off-the-shelf solvers such as CVX [18]. In the remainder of this section, we further show that problem (23) can be transformed into a Stiefel manifold optimization and subsequently solved using the Riemannian conjugate gradient (RCG) method [19]. The latter has been implemented in freely available solvers such as Pymanopt [20].

Recall that constraints $\text{C2} - \text{C4}$ ensure vectors $\vec{\mathbf{q}}_t, \vec{\mathbf{e}}_t$ to be orthonormal. Define $\mathbf{X}_t = [\vec{\mathbf{q}}_t, \vec{\mathbf{e}}_t] \in \mathbb{R}^{3 \times 2}$. We can equivalently rewrite $\text{C2} - \text{C4}$ as

$$\mathbf{X}_t^T \mathbf{X}_t = \mathbf{I}_2. \tag{24}$$

That is, in each frame t, $\mathbf{X}_t$ stays on the Stiefel manifold $\mathcal{M} = \text{St}(p, n)$ with $p = 2$, $n = 3$. Or, in N frames, $\mathbf{X}_t$s lie on a product manifold $\mathcal{N} = \mathcal{M}^N \triangleq \mathcal{M} \times \cdots \times \mathcal{M}$. To exploit the Stiefel manifold structure underlying (23), we now eliminate constraints C5 and C6 from (23) by adding a log-sum-exp penalty function

$$\tilde{f}(\vec{\mathbf{q}}_t, \vec{\mathbf{e}}_t) = \rho \cdot \sum\nolimits_{t=2}^{N} \Big[\alpha \log \big(1 + e^{\frac{\delta_1 - \vec{\mathbf{q}}_t^T \vec{\mathbf{q}}_{t-1}}{\alpha}} \big) + \alpha \log \big(1 + e^{\frac{\delta_2 - \vec{\mathbf{e}}_t^T \vec{\mathbf{e}}_{t-1}}{\alpha}} \big) \Big], \tag{25}$$

into the objective function of (23). Note that $\tilde{f}(\vec{\mathbf{q}}_t, \vec{\mathbf{e}}_t)$ is a smooth or differentiable function, where $\alpha > 0$ is a smoothing parameter and $\rho > 0$ is a penalty factor. With a large ρ and small α, $\tilde{f}(\vec{\mathbf{q}}_t, \vec{\mathbf{e}}_t)$ closely approximates the l_1-norm penalty term $\rho \cdot \sum_{t=2}^{N} \big[\max\{0, \delta_1 - \vec{\mathbf{q}}_t^T \vec{\mathbf{q}}_{t-1}\} + \max\{0, \delta_2 - \vec{\mathbf{e}}_t^T \vec{\mathbf{e}}_{t-1}\}\big]$. The latter is equivalent to C5 and C6. Therefore, problem (23) can be transformed into a standard manifold optimization problem given as

$$\min_{\mathbf{X}_t \in \mathcal{M}} \quad f(\mathbf{X}_t; u_{k,t}, x_{k,t}, \mathbf{w}_{k,t} \mid \vartheta) + \tilde{f}(\mathbf{X}_t). \tag{26}$$

The overall procedure for solving the problem (16) is summarized in Algorithm 1, which has a polynomial-time computational complexity.

Algorithm 1: Proposed BCD Method

Require: $\omega_{k,t}^{(0)}$, $\vec{\mathbf{q}}_t^{(0)}$, $\vec{\mathbf{e}}_t^{(0)}$, $\vartheta^{(0)}$, $\forall k, t$

Ensure: $\mathbf{W}_t^* = [\omega_{1,t}^*, \omega_{2,t}^*, \ldots, \omega_{K,t}^*], \vec{\mathbf{q}}_t^*, \vec{\mathbf{e}}_t^*$, $\forall t \in \mathcal{T}$

$i \leftarrow 1$.
repeat
  Calculate $u_{k,t}^{(i)}$ and $x_{k,t}^{(i)}$ by (20) and (21).
  Solve (22) for given $u_{k,t}^{(i)}, x_{k,t}^{(i)}, \vec{\mathbf{q}}_t^{(i-1)}, \vec{\mathbf{e}}_t^{(i-1)}$ and $\vartheta^{(i-1)}$. Obtain $\mathbf{W}_t^{(i)}$.
  Optimize $\mathbf{X}_t^{(i)}$ in (26) for given $u_{k,t}^{(i)}, x_{k,t}^{(i)}, \mathbf{W}_t^{(i)}$ and $\vartheta^{(i-1)}$. Obtain $\vec{\mathbf{q}}_t^{(i)}, \vec{\mathbf{e}}_t^{(i)}$.
  Update $\vartheta^{(i)} = \sum_{t=1}^{N} \sum_{k=1}^{K} R_{k,t} / P_{\text{tot}}$.
  $i \leftarrow i + 1$.
until Convergence
return $\mathbf{W}_t^{(i-1)}, \vec{\mathbf{q}}_t^{(i-1)}, \vec{\mathbf{e}}_t^{(i-1)}$

V. Simulation Results

In this section, we evaluate the performance of our proposed scheme via simulations. We consider UAV-aided downlink communication over $N = 20$ frames, and each frame spans $\tau = 10$ ms. The operating frequency is set as $f_c = 2.4$ GHz, equivalently the carrier wavelength $\lambda \approx 0.125$ m. The UAV hovers at position $\mathbf{p}_h = [0, 0, 50]^T$m to communicate with $K = 2$ ground users. Unless otherwise specified, we set the maximal angular displacements of both $\vec{\mathbf{q}}_t$ and $\vec{\mathbf{e}}_t$ to be $10°$ per frame, i.e. $\delta_1 = \delta_2 = 0.9848$. For the printed dipole array, the width of the substrate is $D = 60$ millimeter. The number of transmit antennas N_a is specified in each simulation result. The path loss coefficient is $\beta = 10^{-6}$ and the noise power is $\sigma_{k,t}^2 = -90$ dBm, $\forall k, t$. We consider equal transmit power allocation for the users, i.e., $P_k = P_{\max}/K$. Moreover, we

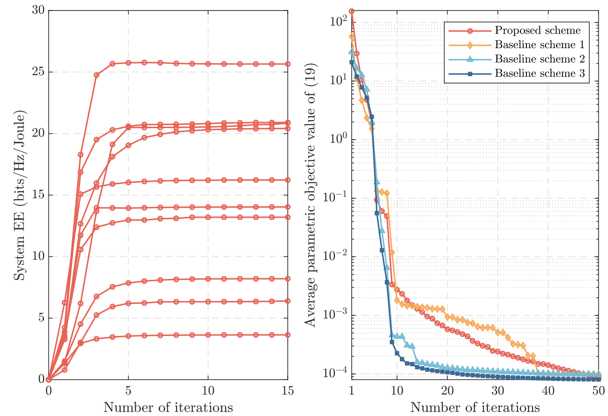

Fig. 3. (Left) System EE versus number of iterations for 10 random instances of problem (16) and (right) average parametric objective value of (19).

set $\eta_m = 0.878$, $\eta_g = 0.72$, $\eta_0 = 0.3$, $P_{\text{stat}} = 40$ dBm, and $P_{\text{SP}} = 10$ dBm for the power consumption model (13). For performance comparison, we consider the following schemes as benchmarks,

- *Baseline Scheme 1:* Joint transmit beamforming and steering optimization for EE maximization, using a ULA of isotropic antennas.
- *Baseline Scheme 2:* Transmit beamforming optimization for EE maximization, using a ULA of dipole antennas.
- *Baseline Scheme 3:* Transmit beamforming optimization for EE maximization, using a ULA of isotropic antennas.
- *Baseline Scheme 4:* Joint transmit beamforming and steering optimization for maximization of sum-SE, using a ULA of dipole antennas.

Baseline Schemes 1 and 4 are also optimized using Algorithm 1 as well, where we set $\rho = 0.02$ and $\alpha = 0.2$.

Fig. 3 validates the convergence of Algorithm 1 by evaluating the system EE for 10 instances of problem (16), and the average parametric objective value of (19) over 100 realizations, where the total transmit power is set to $P_{\max} = 30$ dBm. In each instance or realization, the users' positions and the initial array orientation are randomly generated. We observe that the system EE always converges quickly, within 10 iterations, which confirms its practicality. Meanwhile, the parametric objective value also quickly approaches zero.

Fig. 4 presents a comprehensive performance comparison of the considered schemes in terms of the system EE η_{EE}, the total energy consumption P_{tot}, and the sum-SE $\sum_{t=1}^{N} \sum_{k=1}^{K} R_{k,t}$, for different number of transmit antennas N_a. We observe that Baseline Scheme 4 achieves the highest sum-SE in Fig. 4 (right), but the lowest system EE in Fig. 4 (left) for the considered parameter settings. This is because, by jointly optimizing beamforming and steering using a dipole array to maximize the sum-SE, Baseline Scheme 4 has to consume excessive power for beamforming and array steering, which degrades the system EE. In contrast, by jointly optimizing beamforming and steering of the dipole array for EE maximization, the Proposed Scheme achieves the highest EE for all considered N_as. These results highlight the im-

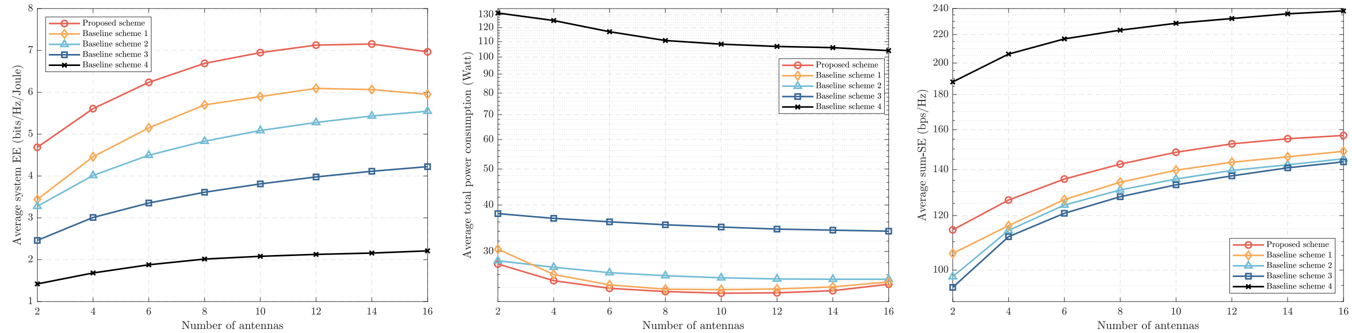

Fig. 4. (Left) Average system EE, (middle) average total power consumption, and (right) average sum-SE versus number of transmit antennas.

portance of EE maximization for UAV-aided communications. Meanwhile, compared to arrays of isotropic antennas (as in Baseline Schemes 1 and 3), the use of dipole arrays (as in the Proposed Scheme and Baseline Scheme 2, respectively) increases both the sum-SE and the system EE for UAV-aided communications, as they can effectively focus the transmit signal towards the users while reducing multiuser interference.

Fig. 4 also shows that the system EE of Baseline Schemes 2–4 monotonically increases with N_a and tends to saturate at large N_a. This is because they can only exploit the optimized beamforming to increase the communication sum-SE, cf. Fig. 4 (right), and at the same time, reduce the transmit power and energy consumption, cf. Fig. 4 (middle). In contrast, there exists an optimal value of N_a, denoted by N_a^*, that maximizes the system EE of the Proposed Scheme and Baseline Scheme 1, where the system EE increases with N_a for $N_a \leq N_a^*$ but decreases for $N_a > N_a^*$. For example, $N_a^* = 14$ and $N_a^* = 12$ for the Proposed Scheme and Baseline Scheme 1, respectively. This is because, unlike the other considered schemes, they consume extra energy for steering the large array as N_a increases, causing their energy consumption to increase with N_a when $N_a \geq 10$. These results imply that simply increasing the number of the transmit antennas may not necessarily improve the system EE, especially for the joint design of array steering and beamforming.

For insights into the performance of the considered schemes, Fig. 5 illustrates their transmit beampattern gains $\sum_{k=1}^{2} |\mathbf{w}_{k,N}^H \mathbf{a}_{k,N}(\theta_{k,N}, \gamma_{k,N})|^2$ in decibels relative to isotropic (dBi). These gains are plotted against the normalized azimuth angle $\gamma_{k,N}$ in radians for each given elevation angle $\theta_{k,N}$, $k = 1, 2$ in frame N. The positions of the users are defined as $\mathbf{p}_1 = [350, -350, 0]$ m and $\mathbf{p}_2 = [200, 200, 0]$ m. The resulting azimuth angles $\gamma_{1,N}$ and $\gamma_{2,N}$ are indicated by dashed lines in Fig. 5. Additionally, for ULAs with isotropic antennas, we have $\theta_{1,N} = \theta_{2,N}$. We observe that in Baseline Schemes 2 and 3, both users share the same azimuth angle. As such, beamforming alone is insufficient to resolve the interference between the users. This decreases the sum-SE, leading to a reduction in the transmit power in order to maximize the system EE. In contrast, the Proposed Scheme and Baseline Scheme 1 utilize the rotatable antenna array to proactively separate the two users from distinct azimuth angles. This effectively mitigates the multiuser interference

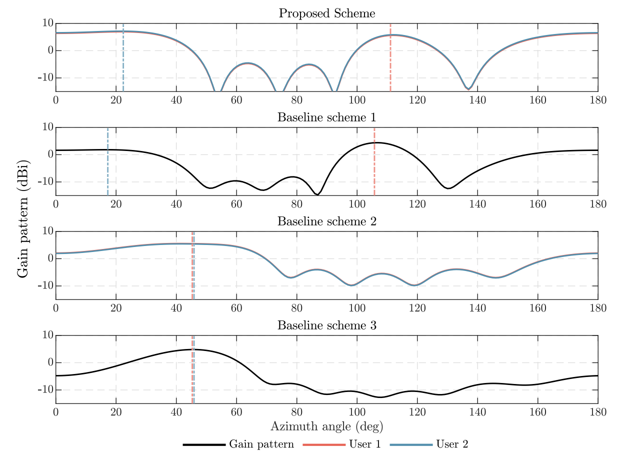

Fig. 5. Gain patterns of considered schemes in frame $N = 20$, with $N_a = 6$.

and, when combined with beamforming, enhances both the sum-SE and the system EE.

Finally, Fig. 6 evaluates the impact of the static power consumption, P_{stat}, on the system EE and the sum-SE. We observe that, for the Proposed Scheme and the Baseline Schemes 1–3, the sum-SE increases with an increasing P_{stat}, at a cost of decreased system EE. This is consistent with the definition of the system EE η_{EE} in (14), because the constant term P_{stat} with large value dominates the total energy consumption in the denominator of η_{EE}. For maximization of η_{EE}, these schemes primarily focus on increasing the sum-SE in the numerator of η_{EE}.

VI. Conclusions

In this paper, we considered energy-efficient UAV-aided multi-user downlink communication by employing a rotatable transmit ULA consisting of dipole antennas. We newly derived an analytical energy consumption model for 3D array steering, based on the kinematics of rigid body. We formulated a nonconvex problem to jointly optimize array steering and transmit beamforming for maximizing the system EE. By reformulating the problem into a parametric optimization, we further proposed a low-complexity proximal BCD algorithm for solution, which involves alternately solving convex optimization and Stiefel manifold optimization subproblems. Simulation results validated the convergence of the proposed algorithm and highlight the superior EE performance gains of joint array steering and beamforming, particularly when

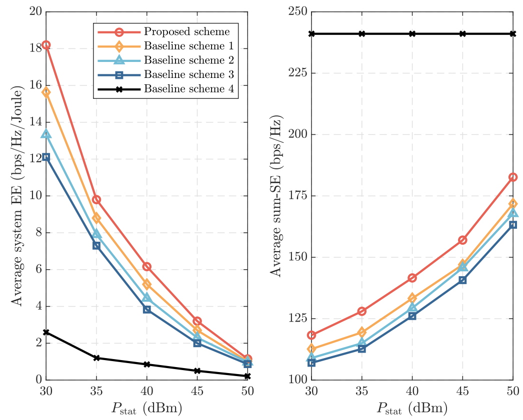

Fig. 6. (Left) Average system EE and (right) average sum-SE versus $P_{\mathtt{stat}}$ over 300 realization for $N = 20$ and $N_a = 6$.

combined with leveraging a dipole array. Additionally, due to trade-offs between SE and energy consumption for joint array steering and beamforming, the number of the transmit antennas should be judiciously optimized when designing energy-efficient UAV-aided communication systems.

References

[1] Q. Wu *et al.*, “A comprehensive overview on 5G-and-beyond networks with UAVs: From communications to sensing and intelligence,” *IEEE J. Sel. Areas Commun.*, vol. 39, no. 10, pp. 2912–2945, 2021.

[2] J. Zhang *et al.*, “Spectrum and energy efficiency maximization in UAV-enabled mobile relaying,” in *IEEE Int. Conf. Commun. (ICC)*, 2017, pp. 1–6.

[3] Y. Su *et al.*, “Spectrum and energy efficiency optimization in IRS-assisted UAV networks,” *IEEE Trans. Commun.*, vol. 70, no. 10, pp. 6489–6502, 2022.

[4] N. Gupta *et al.*, “Trajectory design for throughput maximization in UAV-assisted communication system,” *IEEE Trans. Green Commun. Netw.*, vol. 5, no. 3, pp. 1319–1332, 2021.

[5] X. Jiang *et al.*, “Joint power and trajectory design for UAV-relayed wireless systems,” *IEEE Wireless Commun. Lett.*, vol. 8, no. 3, pp. 697–700, 2019.

[6] X. Huang *et al.*, “Energy consumption optimization for UAV-assisted communication by trajectory design,” in *IEEE Veh. Techn. Conf. (VTC2023-Spring)*, 2023, pp. 1–5.

[7] L. Xiang *et al.*, “Towards power-efficient aerial communications via dynamic multi-UAV cooperation,” in *IEEE Wireless Commun. Netw. Conf. (WCNC)*, 2020, pp. 1–7.

[8] B. Yilmaz *et al.*, “Joint beamforming and trajectory optimization for UAV-aided ISAC with dipole antenna array,” in *Int. Workshop Smart Antennas (WSA)*, 2024.

[9] L. Xiang *et al.*, “Joint optimization of beamforming and 3D array steering for multi-antenna UAV communications,” in *IEEE Wireless Commun. Netw. Conf. (WCNC)*, 2024.

[10] F. Pei *et al.*, “Joint optimization of beamforming and 3D array-steering for UAV-aided ISAC,” in *IEEE Int. Conf. Commun. (ICC)*, 2024.

[11] G. Lu *et al.*, “A global optimization method for energy-minimal UAV-aided data collection over fixed flight path,” in *IEEE Int. Conf. Commun. (ICC)*, 2022, pp. 1220–1226.

[12] X. Cai *et al.*, “A printed dipole array with high gain and endfire radiation,” *IEEE Antennas Wireless Propag. Lett.*, vol. 16, pp. 1512–1515, 2017.

[13] R. A. Serway, *Physics for Scientists and Engineers*. Saunders College Publishing, 1986.

[14] Y. Zeng *et al.*, “Energy minimization for wireless communication with rotary-wing UAV,” *IEEE Trans. Wireless Commun.*, vol. 18, no. 4, pp. 2329–2345, 2019.

[15] J. J. Quispe *et al.*, “RIS-assisted beamforming for energy efficiency in multiuser downlink transmissions,” in *IEEE Globecom Workshops (GC Wkshps)*, 2022, pp. 1543–1548.

[16] W. Dinkelbach, “On nonlinear fractional programming,” *Management Science*, vol. 13, no. 7, pp. 492–498, 1967.

[17] Q. Shi *et al.*, “An iteratively weighted mmse approach to distributed sum-utility maximization for a MIMO interfering broadcast channel,” vol. 59, no. 9, pp. 4331–4340, 2011.

[18] S. Diamond and S. Boyd, “CVXPY: A Python-embedded modeling language for convex optimization,” *J. Machine Learning Research*, vol. 17, no. 83, pp. 1–5, 2016.

[19] X. Yu *et al.*, “MISO wireless communication systems via intelligent reflecting surfaces,” in *IEEE/CIC Int. Conf. Commun. in China (ICCC)*, 2019, pp. 735–740.

[20] J. Townsend *et al.*, “Pymanopt: A python toolbox for optimization on manifolds using automatic differentiation,” *J. Machine Learning Research*, vol. 17, no. 137, p. 1–5, 2016.